polarizations obtained with the two potentials would not necessarily be physically significant.

(α,n) Reactions in Some Elements in the Region of $A = 100$*

LUISA F. HANSEN AND MARION L. STELTS

Lawrence Radiation Laboratory, University of California, Livermore, California

(Received 13 July 1964)

Absolute (α, n) cross sections and angular distributions from 0 to 160° have been measured for Y, Nb, Rh, Ag, Ag[109], and In, from 12 to 18 MeV. The angular distributions show almost complete isotropy, with a systematic trend toward a forward peaking never larger than 5 to 10%. Since, in these elements, neutron emission is expected to be the main contribution to the reaction cross section, the measured (α, n) cross sections have been compared with the predictions of the optical model. Different optical-model potentials for α particles have been tried. Very good agreement with the experimental results has been obtained with the "Igo potential." Reaction cross sections for a square-well potential following Shapiro's calculation for a radius $(1.7\,A^{1/3}+1.21)$ F appear to be in the right order of magnitude, but they do not reproduce the dependence of the excitation function on the incident α energy.

INTRODUCTION

TOTAL reaction cross sections for α particles from 0 to 46 MeV have been predicted by Igo et al.[1,2] for a wide range of nuclei using an optical model in which the parameters of the complex potential were obtained from the elastic scattering of α particles.[3,4] The experimental information available on α-reaction cross sections has until now been very scarce. Igo[5] has measured the reaction cross section for α particles at 40 MeV. Recently, Stelson et al.[6] have done a systematic study of (α,n) cross sections to 11 MeV from Ni to Ag, setting a lower limit to the α-reaction cross section.

It is of interest to extend these measurements to higher energies and for nuclei where the α cross section for the emission of charged particles is negligible, such that the measured (α,n) cross sections are indeed a check of the predicted total reaction cross sections.

Early work in (α,n) reactions for nuclei of A around 100 was done by Bradt et al.[7] in 1947. They measured the (α,n) and $(\alpha,2n)$ cross sections for Rh[103] and Ag[109]

from 11 to 18 MeV. Goshal[8] in 1948 measured the (α,n), $(\alpha,2n)$ and $(\alpha,3n)$ in natural silver from threshold to 37 MeV, and Temmer[9] in 1949 measured these same cross sections in In[115]. In all these measurements, done by activation, no absolute cross sections were obtained. Furthermore, the use of range-energy calculation, already out of data, makes it difficult to compare their results with theory.

Bleuler et al.[10] in 1953 measured $\sigma(\alpha,n)$ and $\sigma(\alpha,2n)$ in Ag[109] by activation. They are the first ones to give absolute values for the cross sections. In 1955 Porges[11] measured $\sigma(\alpha,n)$, $\sigma(\alpha,2n)$, and $\sigma(\alpha,pn)$ for Ag[107] and $(\alpha,2n)$ and $(\alpha,3n)$ in Ag[109] up to 40 MeV.

In the present work angular distributions and absolute $\sigma(\alpha,n)$ have been measured from 12 to 18 MeV for Y, Nb, Rh, Ag, Ag[109], and In. These cross sections have been compared with the predictions of Igo et al.[1] with very good agreement. Comparisons have also been made with the reaction cross-section calculation using the optical-model parameters given by Glassgold[12] to fit the elastic scattering of α in Ag at 22 MeV and with the parameters used by Bassel[13] to fit $\sigma(\alpha,\alpha')$ in Ni[58].

The calculations of Shapiro et al.[14] for α-reaction cross

* Work done under auspices of the U. S. Atomic Energy Commission.

[1] George Igo, Phys. Rev. **115**, 1665 (1959).

[2] J. R. Huizenga and George Igo, Nucl. Phys. **29**, 462 (1962).

[3] D. D. Kerlee, J. S. Blair, and G. W. Farwell, Phys. Rev. **107**, 1343 (1957).

[4] L. Seidlitz, E. Bleuler, and D. J. Tendam, Phys. Rev. **110**, 682 (1957).

[5] G. Igo and B. D. Wilkins, Phys. Rev. **131**, 1251 (1963).

[6] P. H. Stelson and F. K. McGowan, Phys. Rev. **133**, B911 (1964).

[7] H. L. Bradt and D. J. Tendam, Phys. Rev. **72**, 117 (1947).

[8] S. A. Ghoshal, Phys. Rev. **73**, 417 (1948).

[9] G. M. Temmer, Phys. Rev. **76**, 424 (1949).

[10] E. Bleuler, A. K. Stebbins, and D. J. Tendam, Phys. Rev. **90**, 460 (1953).

[11] K. G. Porges, Phys. Rev. **101**, 225 (1956).

[12] W. B. Cheston and A. E. Glassgold, Phys. Rev. **106**, 1215 (1957).

[13] R. H. Bassel, G. R. Satchler, R. M. Drisko, and E. Rost, Phys. Rev. **128**, 2693 (1962).

[14] M. M. Shapiro, Phys. Rev. **90**, 171 (1953).

sections using a square-well potential of radius $(r_0 A^{1/3} + \rho)$ for $r_0 = 1.3$ and 1.5 F and $\rho = 1.21$ F have been shown to give too low values.[5] Calculations were done here for $r_0 = 1.65$ and 1.7 F. The cross sections obtained are in fair agreement with the experimental values above 15 MeV, but they are too high for the lower energies, proving once more that the square-well potential is not suited to fit the excitation function for α particles, because it does not reproduce the proper dependence on the incident energy.

EXPERIMENTAL PROCEDURE

Eight polyethylene "long counters" were used in the measurements of the angular distributions. The counters were built following the DePangher[15] model, with only minor modifications.

Fifteen angles in the interval from 0 to 160° were measured in two steps: 0, 20, 40, 60, 90, 120, 140, and 160°, followed by measurements at 10, 30, 50, 70, 90, 110, 130, and 150°. The counter at 90° was kept fixed between the two sets of measurements to detect any variation that could occur during the two runs. The angular spread at each angle was 2.5°.

The response of the counters to monoenergetic neutrons was measured using the $\mathrm{D}(d,n)\mathrm{He}^3$ reaction and calibrated neutron sources of known energy. Figure 1 shows the efficiency of these polyethylene long counters versus neutron energy.

The target chamber used was a stainless-steel spherical shell, 0.055 in. thick, which has a very uniform transmission of the neutrons at all angles. The targets are mounted on two concentric rings inside the chamber. The target position could be remotely controlled. A total of 12 targets can be mounted at each run.

The efficiency of the entire system at each angle was measured using a standard PoBe source calibrated by the National Bureau of Standards. The bare PoBe sphere, about 1 cm in diam, was mounted at the center of the target holder in the chamber and the neutron flux measured at all angles. The targets used were free foils whose thickness varied between 1 and 2 mg/cm², except for Rh where the thickness was 7.56 mg/cm².
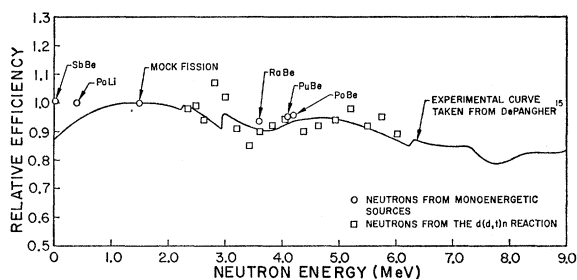
The errors quoted in the measurement of the cross

sections are not larger than 10%, the relative error in the differential cross sections is less than 5%.

RESULTS AND DISCUSSION

Figure 2 shows a typical result of the angular distribution obtained for the neutrons. They are quite isotropic. A systematic trend toward a small forward peaking, between 5 and 10% larger than the flat cross section, can be observed in all of them. Although this increase of the cross sections at the forward angles is inside the errors in the measurements, the contribution from high-energy neutrons at the small angles resulting from direct reaction mechanism cannot be ignored, especially when one sees in Fig. 1 that the efficiency of detection of the system goes down as neutron energy increases.

Neutrons from the direct (α,n) interaction will have average energies between 6 and 10 MeV for the energy range of this work. [The Q values for the (α,n) reactions in these nuclei go from -6.5 MeV in Ag^{109} to -7.7 MeV in Ag^{107} and In.] The efficiency of the long counter for an 8-MeV neutron is around 80% (see Fig. 1). Since the calibration for the absolute cross sections has been done with 4.2-MeV neutrons from the PoBe source, the cross sections for these high-energy neutrons, if present, have been underestimated as much as 15%.

The energy of the incident α particle was determined using the range-energy curves (unpublished; obtained from H. Conzett, Lawrence Radiation Laboratory, Berkeley) for Al based on the experimental results of Bichsel.[16] The errors indicated in the energies are due to energy spread in the target.
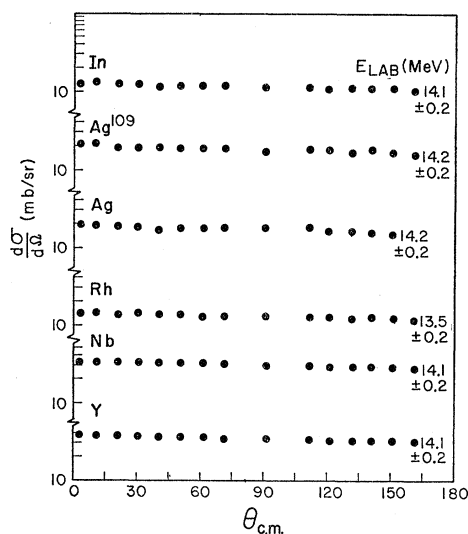

FIG. 2. Angular distributions in the center-of-mass system for neutrons from the (α,n) reactions in In, Ag^{109}, Ag, Rh, Nb, and Y.

FIG. 1. Efficiency of detection of the polyethylene long counter versus neutron energy.

[15] J. DePangher, Nucl. Instr. Methods 5, 61 (1959).

[16] H. Bichsel, R. F. Mozley, and W. A. Aron, Phys. Rev. 105, 1788 (1957).

TABLE I. Range of α particles in Al according to the calculations of Bethe (Ref. 17), Sternheimer (Ref. 18), and Bichsel (Ref. 19). $R_\alpha(3.971E_p) = [0.99288R_p(E_p) + 0.296]$ (mg/cm²), where E_p is the energy of the proton and R_p the range of the proton at the energy E_p.

E_α (MeV)	R_{Bethe}	$R_{\text{Sternheimer}}$	R_{Bichsel}
10	15.8	16.8	16.8
11	18.6	19.6	19.6
12	21.3	22.4	22.5
13	24.3	25.5	25.6
14	27.8	28.9	28.8
15	31.3	32.4	32.3
16	34.9	35.9	35.9
17	38.6	39.7	39.7
18	42.6	43.7	43.6
19	46.8	47.9	47.7
20	50.9	52.3	52.0

One of the main problems in comparing results between different experiments comes from the uncertainty in the energy of the α particles because of different range-energy tables used by the experimenters. In Bleuler's work[10] the determination of the energy was based on the range-energy calculations by Bethe[17] in 1949. In order to compare their results for (α,n) in Ag[109] with the present work, Bleuler's energy scale has to be shifted downward about 0.30 MeV on the average. Table I shows the corresponding range of α particles according to Bethe,[17] Sternheimer,[18] and Bichsel[16] between 10 and 20 MeV.
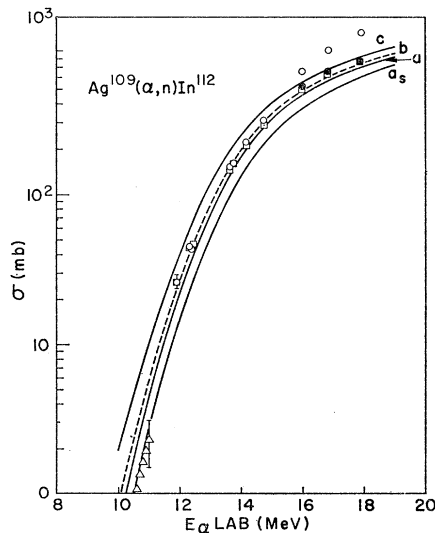

FIG. 3. Absolute cross sections for the reaction Ag[109](α,n)In[112]. Legend: O Measured points; ● Cross sections corrected for $\sigma(\alpha,2n)$; □ measurements of Bleuler et al. (Ref. 10); △ measurements of Stelson et al.; a, reaction cross section for α particles with Igo's potential; a_s, as in a, with a surface absorption potential with Igo's parameters; b, as in a, with Bassel's potential (Ref. 13); c, as in a, with Glassgold's potential (Ref. 12).

[17] Hans A. Bethe, Brookhaven National Laboratory Report BNL-T-7, 1949 (unpublished).
[18] R. M. Sternheimer, Phys. Rev. **115**, 137 (1959).

Figure 3 shows the absolute cross sections for Ag[109](α,n)In[112]. The agreement with Bleuler et al.[10] is quite good once their energy scale has been adjusted according to Bichsel's range-energy scale.

For energy of the particles above 15 MeV neutron contributions from the $(\alpha,2n)$ reaction start to come in for all the nuclei here studied. (Q values have been taken from Nuclear Data Tables.[19]) For Ag[109] the Q value for $(\alpha,2n)$ is 14.44 MeV. The measurements obtained with the "long counter" above this energy were corrected by direct subtraction of the absolute cross section for Ag[109]$(\alpha,2n)$In[111] measured by Bleuler et al.[10]

The thresholds for $(\alpha,2n)$ in Ag[107] and Ag[109] are 16.23 and 14.97 MeV, respectively. The $(\alpha,2n)$ contribution for energies above these thresholds was estimated using the absolute measurements of Refs. 10 and 11. Figure 4 shows the experimental cross sections obtained for Ag(α,n)In.

CALCULATION OF $\sigma(\alpha,2n)$

For Nb, Rh, and In the $(\alpha,2n)$ contribution for energies above the threshold of the reaction had to be calculated. The calculations have been done assuming that the main mechanism for the reaction is compound nucleus formation. (Although this assumption is in part justified because of the isotropy of the angular distributions, it is not a sufficient condition to justify the compound nucleus treatment.) In this case, the contribution from $\sigma(\alpha,2n)$ is given according to Blatt and Weisskopf[20] by the following expression:

$$\sigma(\alpha,2n) = \sigma_{\text{total}}(\alpha,n)[1 - (1 + \epsilon_c/T) \exp(-\epsilon_c/T)], \quad (1)$$

where ϵ_c is the excess energy above the Q value for the $(\alpha,2n)$ reaction and T is the temperature of the intermediate residual nucleus B in the reaction $A(\alpha,n)B$.

The total cross section for the emission of neutrons, $\sigma(\alpha,n)$ total is defined as

$$\sigma_{\text{total}}(\alpha,n) = \sigma_{\text{true}}(\alpha,n) + \sum_i \sigma(\alpha,n,i). \quad (2)$$

For the nuclei here studied, in the energy region of this work the main contribution to the sum term comes from $\sigma(\alpha,2n)$. In this case the cross section measured by the long counter ($\sigma_{\text{LC}}(\alpha,n)$) will be

$$\sigma_{\text{LC}}(\alpha,n) = \sigma_{\text{true}}(\alpha,n) + 2\sigma(\alpha,2n). \quad (3)$$

From Eqs. (1), (2), and (3), one obtains

$$\sigma(\alpha,2n) = \sigma_{\text{LC}}(\alpha,n)K/(1+K),$$

$$\sigma_{\text{total}}(\alpha,n) = \sigma_{\text{LC}}(\alpha,n)/(1+K),$$

where K is given by the square bracket in Eq. (1).

[19] L. A. Koenig, J. H. E. Mattauch, and A. H. Wapstra, *Nuclear Data Tables*, compiled by K. Way et al. (Printing and Publishing Office, National Academy of Sciences—National Research Council, Washington 25, D. C., 1960).
[20] J. M. Blatt and V. F. Weisskopf, *Theoretical Nuclear Physics* (John Wiley & Sons, Inc., New York, 1954), p. 379.

To calculate K it was necessary to know the temperature T. Inasmuch as measurements with the long counter do not give T, its value was taken from the work of Bleuler et al.[10] By comparing the experimental values for the ratio $\sigma(\alpha,2n)/\sigma(\alpha,n)$ with the theoretical predictions of the evaporation model [for a level density of the form $\omega(E) = \text{const} \times \exp(2(aE)^{1/2})$ with $a = 2.5$] they obtained a dependence of the temperature on the energy of the α particles from 1.7 to 2.2 MeV for alpha energies between 14.3 and 18.8 MeV.

This dependence of the temperature on the incident energy of the α particle has also been observed in (α,p) reactions by Lassen and Sidorov[21] and by Swenson and Cindro.[22] Sidorov[23] has measured (α,n) cross sections in medium nuclei and observed a variation of T from 1.2 to 1.5 MeV for α energies of 13.6 to 19.6 MeV. Table II
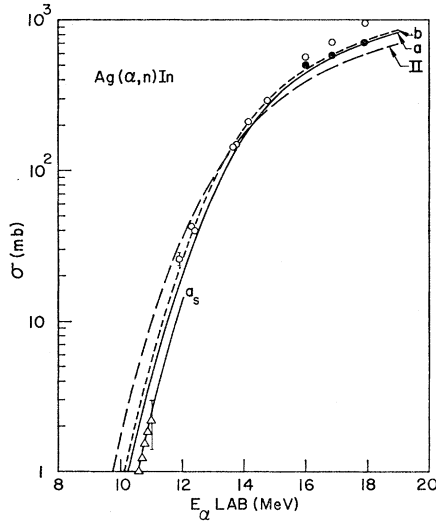

FIG. 4. Absolute cross sections for the reaction $Ag(\alpha,n)In$. Legend: O Measured points; ● cross sections corrected for $\sigma(\alpha,2n)$; △ measurements of Stelson et al.; a, reaction cross sections for α particles with Igo's potential; a_s, as in a with a surface absorption potential with Igo's parameter; b, as in a with Bassel's (Ref. 13) potential; II, as in a with a square-well potential of radius $R = (1.7A^{1/3} + 1.21)$ F.

shows the measured (α,n) cross sections and the calculated $(\alpha,2n)$ cross sections. From the method used to estimate the $\sigma(\alpha,2n)$, the errors in $\sigma_{\text{total}}(\alpha,n)$ above the threshold for $(\alpha,2n)$ production can be as large as 20%.

OPTICAL-MODEL REACTION CROSS SECTIONS

The reaction cross sections predicted by the optical model are a function of the parameters used in the potential. The values of these parameters are obtained, in general, from fitting the angular distributions in the

[21] N. O. Lassen and V. A. Sidorov, Nucl. Phys. **19**, 579 (1960).
[22] W. Swenson and N. Cindro, Phys. Rev. **123**, 910 (1961).
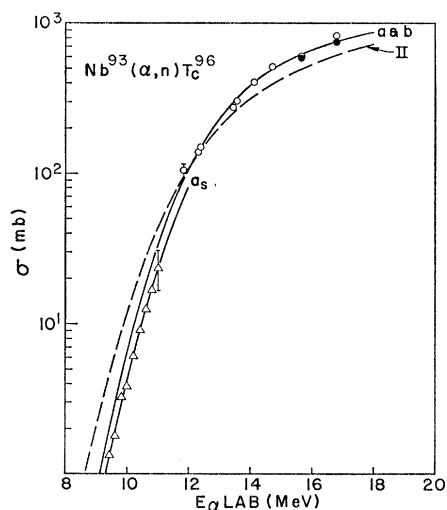[23] V. A. Sidorov, Nucl. Phys. **35**, 253 (1962).

TABLE II. Measured (α,n) cross sections for Y, Nb, Rh, Ag, Ag^{109}, and In and the calculated $(\alpha,2n)$ cross sections.

Target	E_α(lab) (MeV)	$\sigma_{LC}(\alpha,n)$ (mb) (measured) $\pm 10\%$	T (MeV)	$\sigma(\alpha,2n)$ (mb) (calculated)
$_{39}Y^{89}$	10.46±0.2	33.2		
	11.83±0.2	137		
	12.31±0.2	177		
	13.55±0.2	356		
	14.07±0.2	415		
$_{41}Nb^{93}$	11.86±0.2	105		
	12.35±0.2	140		
	12.39±0.3	151		
	13.45±0.3	273		
	13.58±0.2	302		
	14.11±0.2	403		
	14.79±0.3	433		
	15.67±0.3	587	1.8	9.0
	16.81±0.3	830	1.86	81
$_{45}Rh^{103}$	11.22±0.3	17.5		
	11.63±0.3	27.3		
	11.74±0.3	29.6		
	12.99±0.3	114		
	13.12±0.3	112		
	13.53±0.3	172		
	14.12±0.3	231		
	15.42±0.3	426		
	16.29±0.3	558	1.85	5.0
	17.40±0.3	818	1.95	87
$_{47}Ag$	11.92±0.2	26.0		
	12.31±0.2	42.9		
	12.40±0.2	40.2		
	13.63±0.2	145		
	13.75±0.2	150		
	14.15±0.2	212		
	14.72±0.2	292		
	15.99±0.2	576		62.2[a] 58.3[b]
	16.84±0.2	720	1.87	11.0+118[a] 40.1+117[b]
	17.92±0.2	995	1.94	74.0+200[a] 107 +187[b]
$_{47}Ag^{109}$	11.92±0.2	26.0		
	12.31±0.2	44.4		
	12.40±0.2	42.9		
	13.62±0.2	153		
	13.74±0.2	158		
	14.15±0.2	220		
	14.72±0.2	308		
	15.99±0.2	540		128[a], 120[b]
	16.83±0.2	901		243[a], 240[b]
	17.91±0.2	1186		412[a], 385[b]
$_{49}In^{115}$	11.91±0.2	9.83		
	12.39±0.2	16.7		
	13.62±0.2	91.0		
	13.72±0.2	99.7		
	14.14±0.2	138		
	14.70±0.2	227		
	15.96±0.2	391	1.72	30
	16.81±0.2	597	1.83	112
	17.89±0.2	858	1.95	246

[a] Sum of $\sigma(\alpha,2n)$ for Ag^{107} and Ag^{109} from Ref. 10.
[b] Sum of $\sigma(\alpha,2n)$ for Ag^{107} and Ag^{109} from Ref. 11.

elastic scattering process. Frequently, there are more than one set of parameters that fit the elastic-scattering data equally well. In that case the choice of the "best set of parameters" has to be made using additional experimental information, such as reaction cross sections, inelastic scattering, or polarization measurements.

FIG. 5. Absolute cross sections for the reaction $Nb^{93}(\alpha,n)Tc^{96}$. Legend: ○ Measured points; ● cross sections corrected for $\sigma(\alpha,2n)$; △ measurements of Stelson et al; a, reaction cross sections for α particles with Igo's potential; a_s as in a with a surface absorption potential with Igo's parameter; b, as in a with Bassel's (Ref. 13) potential; II, as in a with a square-well potential of radius $R=(1.7A^{1/3}+1.21)$ F.

It has been argued by Satchler[24] that this would not be so if high-accuracy differential cross sections for elastic scattering were measured. In this case, a unique set of model parameters could be obtained. However, this will require experimental measurements with errors no larger than 1 to 2%.
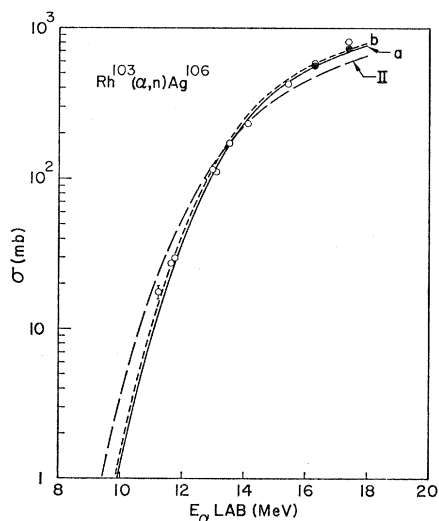

FIG. 6. Absolute cross sections for the reactions $Rh^{103}(\alpha,n)Ag^{106}$. Legend: ○ Measured points: ● corrected for $\sigma(\alpha,2n)$; a, reaction cross sections for α particles with Igo's potential; b, as in a with Bassel's potential (Ref. 13); II, as in a with a square-well potential of radius $R=(1.7A^{1/3}+1.21)$ F.

[24] G. R. Satchler, *Direct Interactions and Nuclear Reactions Mechanisms* (Gordon and Breach Science Publishers, New York, 1963), p. 93.
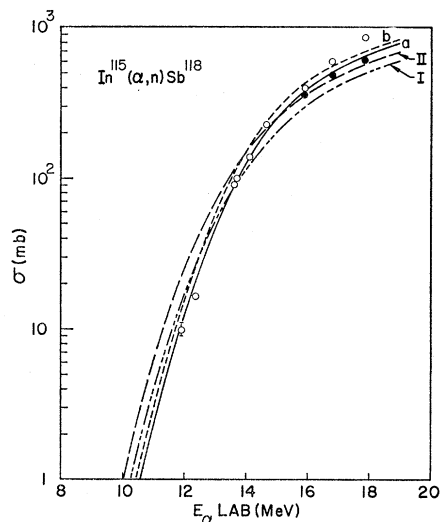

FIG. 7. Absolute cross sections for the reactions $In^{115}(\alpha,n)Sb^{118}$. Legend: ○ Measured points; ● corrected for $\sigma(\alpha,2n)$; a, reaction cross sections for α particles with Igo's potential; b, as in a with Bassel's potential (Ref. 13); I, as in a with a square-well potential of radius $R=(1.65A^{1/3}+1.21)$ F; II, as in a with a square-well potential of radius $R=(1.7A^{1/3}+1.21)$ F.

With this in mind, a comparison has been made in this work between the reaction cross section for α particles predicted by the optical model for different sets of parameters and the measured values of (α,n) cross sections. The reaction cross sections calculated using Igo's potential are in very good agreement with the measured values for Nb^{93}, Rh^{103}, and In^{115}, as can be seen in Figs. 5, 6, and 7.

The (α,n) cross sections for Nb^{93} below 11 MeV shown in Fig. 5 are the measurements of Stelson et al.,[5]

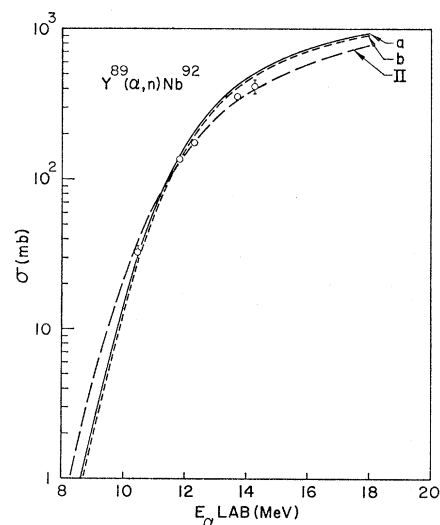FIG. 8. Absolute cross sections for the reaction $Y^{89}(\alpha,n)Nb^{92}$. Legend: ○ Measured points; ● corrected for $\sigma(\alpha,2n)$; a reaction cross sections for α particles with Igo's potential; b as in a with Bassel's potential (Ref. 13); II as in a with a square-well potential of radius $R=(1.7A^{1/3}+1.21)$ F.

TABLE III. Optical-model parameters used in the calculations of the α-reaction cross sections.

Nuclei	V (MeV) I[a]	II[b]	III[c]	W (MeV) I	II	III	a (F) I	II	III	b (F) I	r₀ (F) I	II	III	ρ (F) I	II	III
$_{39}Y^{89}$	−50	−47.6	−50	−13.5	−13.8		0.576	0.549	0.600	1.00	1.17	1.585	1.58	1.77	0	0
$_{41}Nb^{93}$	−50	−47.6	−50	−13.7	−13.8		0.576	0.549	0.600	1.00	1.17	1.585	1.58	1.77	0	0
$_{45}Rh^{103}$	−50	−47.6	−50	−14.3	−13.8		0.576	0.549	0.600	1.00	1.17	1.585	1.58	1.77	0	0
$_{47}Ag^{107.9}$	−50	−47.6	−50	−14.8	−13.8		0.576	0.549	0.600	1.00	1.17	1.585	1.58	1.77	0	0
$_{47}Ag^{109}$	−50	−47.6	−50	−14.9	−13.8	−20.0	0.576	0.549	0.600	1.00	1.17	1.585	1.58	1.77	0	0
$_{49}In^{115}$	−50	−47.6	−50	−15.7	−13.8		0.576	0.549	0.600	1.00	1.17	1.585	1.58	1.77	0	0

[a] Refs. 1, 2.   [b] Ref. 13.   [c] Ref. 12.

and are lower than the predicted values. The solid curve through these points represents the reaction cross sections calculated using Igo's parameters for a surface absorption potential. These cross sections are lower than those calculated with Igo's potential, which is a volume absorption potential.

$$V_{\text{volume}} = -(V + iW)f(r),$$

where $f(r) = \{1 + \exp[(r-R)/a]\}^{-1}$;

$$V_{\text{surface}} = -Vf(r) - iWg(r),$$

where $g(r) = \exp[-(r-R)/b]^2$.

If this is a real effect, it will suggest that the optical-model potential for α particles, as in the case of protons,[25] is a mixture of surface and volume absorption, with the volume absorption increasing as the energy of the incident α particle increases.

Figure 8 show the results for Y^{89}. At the higher energies, the measured (α,n) cross sections are smaller than the calculated ones. A possible reason for this effect is that since Y^{89} is a lower Z element, the charged-particle contribution to the reaction cross section starts to be important at the higher energies, and $\sigma(\alpha,n)$ will give only the lower limit to the reaction cross section. The calculated reaction cross sections for Ag^{109} and natural silver are shown in Figs. 3 and 4.

Cheston and Glassgold[12] compared the elastic scattering of α particles on Ag at 22 MeV with a volume absorption optical potential, with the parameters shown in Table III. The reaction cross sections calculated with this potential are shown in Fig. 3. They are systematically larger than the calculated cross sections using Igo's potential.

[25] J. S. Nodvik, C. B. Duke, and M. A. Melkanoff, Phys. Rev. 125, 975 (1962).

Recently, Bassel et al.[13] have fitted elastic and inelastic scattering of 43-MeV α particles from Ni^{58} and Ni^{60} using also a volume absorption potential with the parameters shown in Table III. Using these parameters, the reaction cross sections were calculated for all the nuclei here studied. They compared very closely with Igo's calculations. Bassel's potential has the attractive feature of having a single set of parameters, while in Igo's potential the depth of the imaginary potential is an increasing function of the atomic number. To make a choice between the two potentials, one must analyze the α-particle elastic scattering from these nuclei with Bassel's potential to see if the fits are equally good or better than the ones obtained with Igo's potential.

The reaction cross section for α particles as predicted by Shapiro for a square-well potential using a radius of $(r_0 A^{1/3} + 1.21)$ F for $r_0 = 1.65$ and 1.7 F are shown in Fig. 7. It has been shown previously[6,10] that Shapiro's calculations[13] for $r_0 = 1.5$ and 1.3 F give cross sections too low compared with the measured values. $R = (1.7 A^{1/3} + 1.21)$ F is the radius that seems to fit better some of the experimental results at some energies, as can be seen from Figs. 3 to 8. However, the main objection to the Shapiro calculation is not the magnitude of the radial parameter r_0, but that it does not reproduce the dependence of the reaction cross sections on the energy of the incident α particle.

ACKNOWLEDGMENTS